6-10-2011

Dynamics of entanglement in a two-dimensional spin system

Qing Xu
Purdue University

Gehad Sadiek
Al Qasseem University; King Saud University; Ain Shams University

Sabre Kais
Birck Nanotechnology Center, Purdue University; Al Qasseem University; King Saud University, kais@purdue.edu

Dynamics of entanglement in a two-dimensional spin system

Qing Xu,[1] Gehad Sadiek,[2,3] and Sabre Kais[2,4,*]

[1]*Department of Physics, Purdue University, West Lafayette, Indiana 47907, USA*

[2]*Department of Physics, King Saud University, Riyadh 11451, Saudi Arabia*

[3]*Department of Physics, Ain Shams University, Cairo 11566, Egypt*

[4]*Department of Chemistry and Birck Nanotechnology Center, Purdue University, West Lafayette, Indiana 47907, USA*

(Received 30 January 2011; published 10 June 2011)

We consider the time evolution of entanglement in a finite two-dimensional transverse Ising model. The model consists of a set of seven localized spin-$\frac{1}{2}$ particles in a two-dimensional triangular lattice coupled through nearest-neighbor exchange interaction in the presence of an external time-dependent magnetic field. The magnetic field is applied in different function forms: step, exponential, hyperbolic, and periodic. We found that the time evolution of the entanglement shows an ergodic behavior under the effect of the time-dependent magnetic fields. Also, we found that while the step magnetic field causes great disturbance to the system, creating rapid oscillations, the system shows great controllability under the effects of the other magnetic fields where the entanglement profile follows closely the shape of the applied field even with the same frequency for periodic fields. This follow-up trend breaks down as the strength of the field, the transition constant for the exponential and hyperbolic forms, or the frequency for periodic field increase leading to rapid oscillations. We observed that the entanglement is very sensitive to the initial value of the applied periodic field: the smaller the initial value is, the less distorted the entanglement profile is. Furthermore, the effect of thermal fluctuations is very devastating to the entanglement, which decays very rapidly as the temperature increases. Interestingly, although a large value of the magnetic field strength may yield a small entanglement, the magnetic field strength was found to be more persistent against thermal fluctuations than the small field strengths.

DOI: 10.1103/PhysRevA.83.062312 PACS number(s): 03.67.Mn, 03.65.Ud, 75.10.Jm

I. INTRODUCTION

Quantum entanglement lies at the heart of quantum theory and has a fundamental role in modern physics [1]. Entanglement is a nonlocal correlation between two (or more) quantum systems such that the description of their states has to be done with reference to each other even if they are spatially well separated. Understanding and quantifying entanglement may provide an answer for many questions regarding the behavior of complex quantum systems [2]. Particularly, entanglement is considered to be the physical property responsible for the long-range quantum correlations accompanying a quantum phase transition in many-body systems at zero temperature [3–7]. Particular fields where entanglement plays a crucial role are quantum teleportation, quantum cryptography, and quantum computing, where it is considered to be the physical basis for manipulating linear superpositions of the quantum states to implement the different proposed quantum computing algorithms [8,9]. Different physical systems have been proposed as reliable candidates for the future technology of quantum computing and quantum-information processing [10–17]. The main task in each one of these systems is to specify a certain quantum degree of freedom as the qubit and to find a controllable coupling mechanism to form an entanglement among these qubits to perform efficient quantum computing processes.

Multiparticle systems are of central interest in the field of quantum information, in particular, quantification of the entanglement contained in their quantum states. However, quantum states and entanglement are very fragile due to the induced decoherence caused by the inevitable coupling to the environment. Decoherence is considered to be one of the main obstacles toward realizing an effective quantum computing system [18]. The main effect of decoherence is to randomize the relative phases of the possible states of the considered system. Quantum error correction [19] and decoherence-free subspace [20,21] have been proposed to protect the quantum property during the computation process. Still, offering a potentially ideal protection against environmentally induced decoherence is difficult. In NMR quantum computers, a series of magnetic pulses were applied to a selected nucleus of a molecule to implement quantum gates [22]. Moreover, a spin-pair entanglement is a reasonable measure for decoherence between the considered two-spin system and the environmental spins. The coupling between the system and its environment leads to decoherence in the system and vanishing of entanglement between the two spins. Evaluating the entanglement remaining in the considered system helps us to understand the behavior of the decoherence between the considered two spins and their environment [23].

In previous works, the evolution of entanglement in a one-dimensional spin system in the presence of different forms of external magnetic fields, modeled by the XY Hamiltonian, was studied [24,25]. It was found that the entanglement can be localized between nearest-neighbor qubits for certain values of the external time-dependent magnetic fields. Moreover, as known for the magnetization of this model, the entanglement showed nonergodic behavior, i.e., it does not approach its equilibrium value at the infinite time limit. Also, the same system was investigated considering a time-dependent exchange coupling between neighboring spins [26]. It was found that the asymptotic behavior of entanglement at the infinite time

*kais@purdue.edu

limit is very sensitive to the initial values of the coupling and magnetic field, and for particular choices we may create finite asymptotic entanglement regardless of the final values of coupling and magnetic field. The quantum effects in the Ising model case showed persistence in the vicinity of both its critical phase transition point and zero temperature as it evolves in time.

The study of quantum entanglement in two-dimensional systems possesses a number of extra problems compared with systems of one dimension. A particular problem is the lack of exact solutions. The existence of exact solutions has contributed enormously to the understanding of the entanglement for 1D systems [24,26–28]. Studies can be carried out on interesting but complicated properties, can be applied to infinitely large systems, and thus can use the finite scaling method to eliminate the size effects, etc. Some approximation methods, such as the density matrix renormalization group (DMRG), are also only workable in one dimension [22,29–31]. So when we carry out this two-dimensional study, no methods can be taken from previous studies. They heavily rely on numerical calculations, resulting in severe limitations on the system size and properties. For example, dynamics of the system is a computationally costly property. We have to think of a way to improve the effectiveness of computation in order to increase the size of research objects while digging the physics in the observable systems. It may show the general physics or tell us the direction of less costly large-scale calculations. In a previous work we studied the entanglement in a 19-site two-dimensional transverse Ising model at zero temperature [32]. The spin-$\frac{1}{2}$ particles were coupled through an exchange interaction J and subject to an external time-independent magnetic field h. We demonstrated that for such a class of systems the entanglement can be tuned by varying the parameter $\lambda = h/J$ and also by introducing impurities into the system. The system showed a quantum phase transition at a specific critical value of the parameter λ_c.

In this paper, we consider the dynamics of entanglement in a two-dimensional spin system, where spins are coupled through an exchange interaction and subject to an external time-dependent magnetic field. Four forms of time-dependent magnetic field are considered: step, exponential, hyperbolic, and periodic. To tackle the problem, we introduce two calculation methods: step-by-step time-evolution matrix transformation and step-by-step projection. We compare them side by side; in short, in addition to having the exact same results, the step-by-step projection method turned out to be 20 times faster than the matrix transformation. One section of this paper will discuss the scalability of this method and shed light on studies of larger systems. The finite-temperature effect is also considered to simulate more realistic systems. We show that the system entanglement behaves in an ergodic way in contrary to the one-dimensional Ising system. The system shows great controllability under all forms of external magnetic field except the step function one, which creates rapidly oscillating entanglement. This controllability is shown to be breakable as the different magnetic field parameters increase. Also, it will be shown that the mixing of even a few excited states by small thermal fluctuation is devastating to the entanglement of the ground state of the system. The critical temperature at which the concurrence vanishes depends significantly on the value of the magnetic field strength: a smaller value yields smaller entanglement but higher critical temperature.

This paper is organized as follows. In the next section we present our model and discuss the two different approaches to evaluate the entanglement. In Sec. III we present and discuss our results for the entanglement of the system under the effects of the different magnetic fields forms at zero temperature. The dynamics of thermal entanglement is considered in Sec. IV. In Sec. V we explain part of our key results in light of Fermi's golden rule and adiabatic approximation. The extension of our work to larger-size spin systems is discussed in Sec. VI. We conclude in Sec. VII and discuss future directions.

II. SOLUTION OF THE TIME-DEPENDENT TWO-DIMENSIONAL ISING MODEL

A. Model

We consider a set of seven localized spin-$\frac{1}{2}$ particles in a two-dimensional triangular lattice coupled through exchange interaction J and subject to an external time-dependent magnetic field of strength $h(t)$. The Hamiltonian for such a system is given by

$$H = -\sum_{\langle i,j\rangle} J_{i,j}\sigma_i^x\sigma_j^x - h(t)\sum_i \sigma_i^z, \tag{1}$$

where $\langle i,j\rangle$ is a pair of nearest-neighbor sites on the lattice; $J_{i,j} = J$ for all sites. For this model it is convenient to define a dimensionless coupling constant $\lambda = h/J$. We apply different forms of the magnetic field as a function of time: step function, exponential, hyperbolic, and periodic.

B. The evolution operator

According to quantum mechanics, the transformation of $|\psi_i(t_0)\rangle$, the state vector at the initial instant t_0, into $|\psi_i(t)\rangle$, the state vector at an arbitrary instant, is linear [33]. Therefore there exists a linear operator $U(t,t_0)$ such that

$$|\psi_i(t)\rangle = U(t,t_0)\,|\psi_i(t_0)\rangle. \tag{2}$$

This is, by definition, the evolution operator of the system. Substituting Eq. (2) into the Schrödinger equation, we obtain

$$i\hbar\frac{\partial}{\partial t}U(t,t_0)|\psi(t_0)\rangle = H(t)U(t,t_0)|\psi(t_0)\rangle, \tag{3}$$

which means

$$i\hbar\frac{\partial}{\partial t}U(t,t_0) = H(t)U(t,t_0). \tag{4}$$

Further, taking the initial condition,

$$U(t_0,t_0) = \mathbb{I}, \tag{5}$$

the evolution operator can be condensed into a single integral equation:

$$U(t,t_0) = \mathbb{I} - \frac{i}{\hbar}\int_{t_0}^{t} H(t')U(t',t_0)dt'. \tag{6}$$

When the operator H does not depend on time, Eq. (6) can easily be integrated and finally leads to

$$U(t,t_0) = e^{-iH(t-t_0)/\hbar}. \tag{7}$$

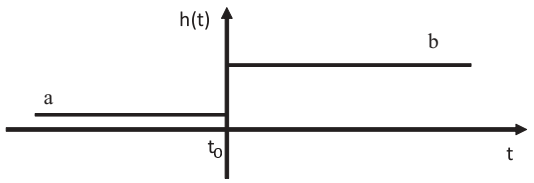

FIG. 1. The external magnetic field in a step function form $h(t) = a$ at $t \leqslant t_0$, $h(t) = b$ at $t > t_0$.

C. Step-by-step time-evolution matrix transformation

To unveil the behavior of concurrence at time t, we need to find the density matrix of the system at that moment, which can be obtained from

$$\rho(t) = U(t)\rho(0)U^{\dagger}(t). \tag{8}$$

Although Eq. (6) gives a beautiful expression for the evolution operator, in reality, U is hard to obtain because of the integration involved. In order to overcome this obstacle, let us first consider the simplest time-dependent magnetic field: a step function of the form (Fig. 1)

$$h(t) = a + (b-a)\theta(t-t_0)\,, \tag{9}$$

where $\theta(t-t_0)$ is the usual mathematical step function defined by

$$\theta(t-t_0) = \begin{cases} 0 & t \leqslant t_0 \\ 1 & t > t_0 \end{cases}. \tag{10}$$

At t_0 and before, the system is time independent since $H_a \equiv H(t \leqslant t_0) = -\sum_{\langle i,j\rangle}\sigma_i^x\sigma_j^x - a\Sigma_i\sigma_i^z$. Therefore we are capable of evaluating its ground state and density matrix at t_0 straightforwardly. For the interval t_0 to t, the Hamiltonian $H_b \equiv H(t > t_0) = -\sum_{<i,j>}\sigma_i^x\sigma_j^x - b\Sigma_i\sigma_i^z$ does not depend on time either, so Eq. (7) enables us to write out

$$U(t,t_0) = e^{-iH(t>t_0)(t-t_0)/\hbar}, \tag{11}$$

and therefore

$$\rho(t) = U(t,t_0)\rho(t_0)U^{\dagger}(t,t_0). \tag{12}$$

Starting from here, it is not hard to think of breaking an arbitrary magnetic function into small time intervals and treating every neighboring intervals as a step function. Comparing the two graphs in Fig. 2, the method has just turned ski sliding into mountain climbing. Assuming each time interval is Δt, setting $\hbar = 1$, then

$$U(t_i,t_0)|\psi_0\rangle = U(t_i,t_{i\text{-}1})U(t_{i\text{-}1},t_{i\text{-}2})\ldots U(t_1,t_0)|\psi_0\rangle, \tag{13}$$

$$U(t_i,t_0) = \prod_{k=1}^{i}\exp[-iH(t_k)\Delta t], \tag{14}$$

$$U(t_i,t_0) = \exp[-iH(t_i)\Delta t]U(t_{i\text{-}1}-t_0). \tag{15}$$

Here we avoided integration; instead, we have chain multiplications that can be easily realized as loops in computational calculations. This is a common numerical technique; the desired precision can be achieved via proper time-step length adjustment.

D. Step-by-step projection

The step-by-step matrix transformation method successfully breaks down the integration but still involves the matrix exponential, which is costly in numerical resources. We propose a projection method to accelerate the calculations. Let us look at the step magnetic field again (Fig. 1). For H_a, after a long enough time, the system at zero temperature is in the ground state $|\phi\rangle$ with energy, say, ε. We want to ask how this state will evolve after the magnetic field is turned to the value b. Assume the new Hamiltonian H_b has N eigenpairs E_i and $|\psi_i\rangle$. The original state $|\phi\rangle$ can be expanded in the basis $\{|\psi_i\rangle\}$:

$$|\phi\rangle = c_1|\psi_1\rangle + c_2|\psi_2\rangle + \cdots + c_N|\psi_N\rangle, \tag{16}$$

where

$$c_i = \langle\psi_i|\phi\rangle. \tag{17}$$

When H is independent of time between t and t_0, then we can write

$$\begin{aligned} U(t,t_0)\,|\psi_{i,t_0}\rangle &= e^{-iH(t>t_0)(t-t_0)/\hbar}|\psi_{i,t_0}\rangle \\ &= e^{-iE_i(t-t_0)/\hbar}|\psi_{i,t_0}\rangle. \end{aligned} \tag{18}$$

Now the exponent in the evolution operator is a number that is no longer a matrix. The ground state will evolve with time as

$$\begin{aligned} |\phi(t)\rangle &= c_1|\psi_1\rangle e^{-iE_1(t-t_0)} + c_2|\psi_2\rangle e^{-iE_2(t-t_0)} + \cdots \\ &\quad + c_N|\psi_N\rangle e^{-iE_N(t-t_0)} = \sum_{i=1}^{N} c_i|\psi_i\rangle e^{-iE_i(t-t_0)}, \end{aligned} \tag{19}$$

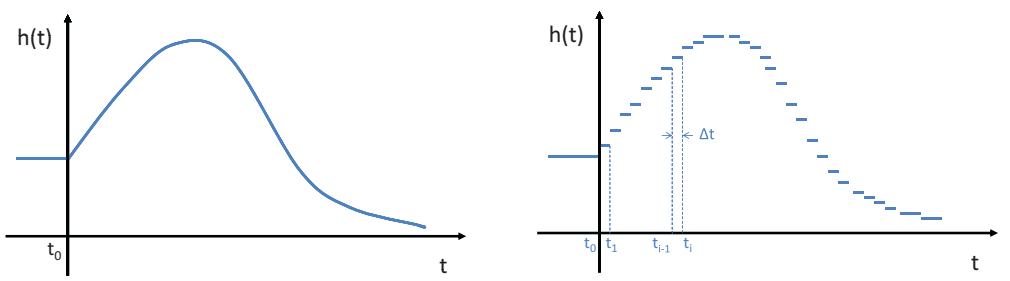

(a) (b)

FIG. 2. (Color online) Divide an arbitrary magnetic field function into small time intervals. Every time step is Δt. Treat the field within the interval as a constant. As a result, we turn a smooth function into a collection of step functions, which makes the calculation of dynamics possible.

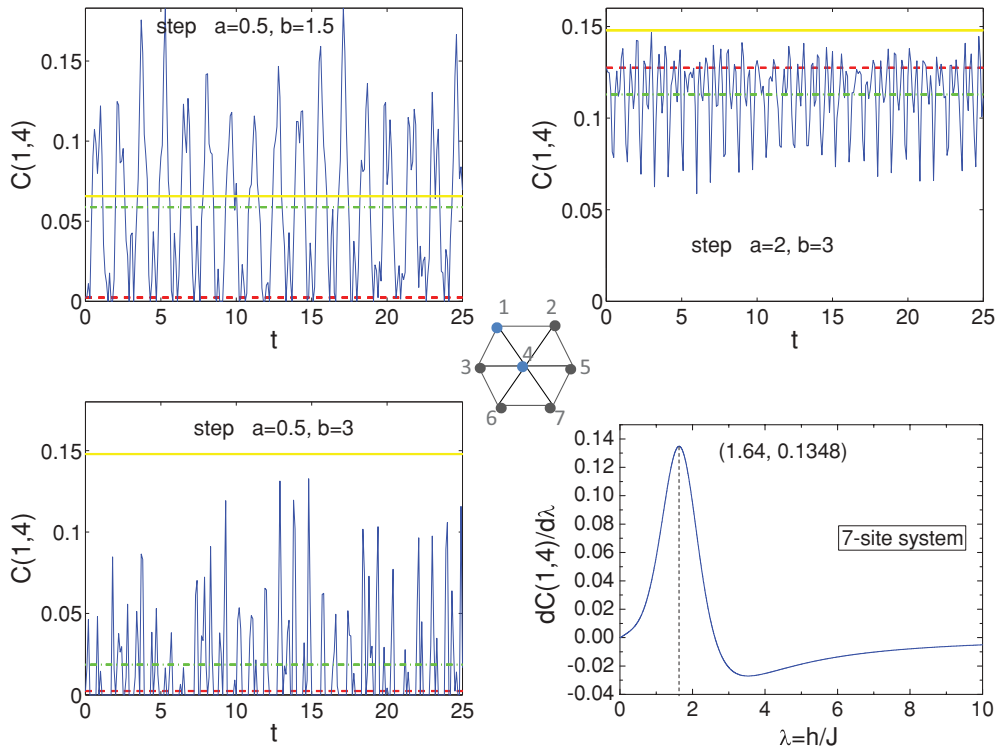

FIG. 3. (Color online) Dynamics of $C(1,4)$ (solid blue line) in the seven-site system when the step magnetic field is changed from $a = 0.5$ to $b = 1.5$ (before the "critical point" $h = 1.64$), from $a = 2$ to $b = 3$ (after), and from $a = 0.5$ to $b = 3$ (big step across the critical point), where time t is in units of J^{-1}, the dashed red line indicates the concurrence corresponding to a constant magnetic field $h = a$, the straight solid yellow line shows $h = b$, and the dot-dashed green line represents the average value of the oscillating concurrence.

and the pure state density matrix becomes

$$\rho(t) = |\phi(t)\rangle\langle\phi(t)|. \tag{20}$$

Again, any complicated function can be treated as a collection of step functions. When the state evolves to the next step, just repeat the procedure to get the following results. Our test shows, for the same magnetic field, that both methods give the same results, but projection is much faster (about 20 times faster) than matrix transformation. This is a great advantage when the system size increases. But this is not the end of the problem. The summation is over all the eigenstates. Extending one layer out to 19 sites, fully diagonalizing the $2^{19} \times 2^{19}$ Hamiltonian, and summing over all of them in every time step is breathtaking. In a later section, we will show how to further improve the method to reduce the number of calculations, which will pave the way toward larger systems.

E. Entanglement of formation

We confine our interest to the entanglement of two spins, at any position i and j [34]. We adopt the entanglement of formation, a well-known measure of entanglement [35], to quantify our entanglement [36]. All the information needed in this case, at any moment t, is contained in the reduced density matrix $\rho_{i,j}(t)$, which can be obtained from the entire system density matrix by integrating out all the spins states except i and j. Wootters [35] has shown that, for a pair of binary qubits, the concurrence C, which goes from 0 to 1, can be taken as a measure of entanglement. The concurrence between sites i and j is defined as

$$C(\rho) = \max\{0, \epsilon_1 - \epsilon_2 - \epsilon_3 - \epsilon_4\}, \tag{21}$$

where ϵ_i are the eigenvalues of the Hermitian matrix $R \equiv \sqrt{\sqrt{\rho}\tilde{\rho}\sqrt{\rho}}$ with $\tilde{\rho} = (\sigma^y \otimes \sigma^y)\rho^*(\sigma^y \otimes \sigma^y)$ and σ^y is the Pauli matrix of the spin in the y direction. For a pair of qubits the entanglement can be written as

$$E(\rho) = \epsilon(C(\rho)), \tag{22}$$

where ϵ is a function of the "concurrence" C,

$$\epsilon(C) = h\left(\frac{1 - \sqrt{1 - C^2}}{2}\right), \tag{23}$$

where h is the binary entropy function

$$h(x) = -x \log_2 x - (1 - x)\log_2(1 - x). \tag{24}$$

In this case, the entanglement of formation is given in terms of another entanglement measure, the concurrence C. The matrix elements of the reduced density matrix needed for calculating the concurrence can be obtained numerically using one of the two methods developed above.

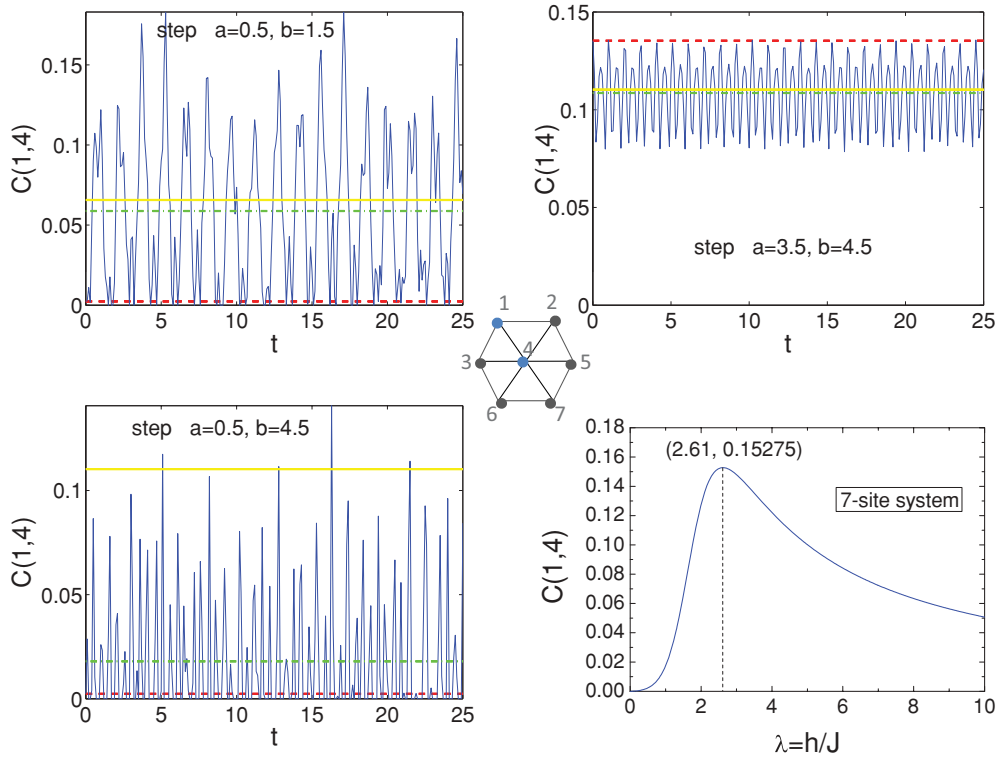

FIG. 4. (Color online) Dynamics of $C(1,4)$ (solid blue line) in the seven-site system when the step magnetic field is changed from $a = 0.5$ to $b = 1.5$ (before the "maximum point" $h = 2.61$), from $a = 3.5$ to $b = 4.5$ (after), and from $a = 0.5$ to $b = 4.5$ (big step across the maximum point), where time t is in units of J^{-1}, the dashed red line indicates the concurrence corresponding to a constant magnetic field $h = a$, the straight solid yellow line shows $h = b$, and the dot-dashed green line represents the average value of the oscillating concurrence.

III. DYNAMICS OF THE SPIN SYSTEM IN A TIME-DEPENDENT MAGNETIC FIELD

A. Step magnetic field

First, we study the dynamic response of the seven-site spin system to the external step magnetic field (Fig. 1), the simplest form of the time-dependent function, which is given by

$$h(t) = a + (b - a)\theta(t - t_0)\ . \tag{25}$$

In previous work we showed that this two-dimensional spin system has a critical point at $\lambda = 1.64$ and a maximum reachable concurrence at $\lambda = 2.61$ [32]. Accordingly, we design here all kinds of steps, big, small, jump, drop, and happening before, after, or across the "critical point" (and "maximum point"), trying to identify what will affect the system behavior and how.

Figure 3 displays the dynamics of the pairwise entanglement between sites 1 and 4, $C(1,4)$, when the magnetic field is changed from $a = 0.5$ to $b = 1.5$ (before the critical point $h = 1.64$), from $a = 2$ to $b = 3$ (after), and from $a = 0.5$ to $b = 3$ (big step across the critical point). Thick and big oscillations appear in every graph. Dynamics of $C(1,4)$ under similar design (Fig. 4) but before, after, and across the maximum point $h = 2.61$ shows similar oscillations. In Figs. 3 and 4, we have plotted the concurrence corresponding to a constant magnetic field $h = a$ (red dashed line), $h = b$ (straight yellow solid line), and the average value of the oscillating concurrence (green dot-dashed line). In the same manner, the dynamics of the concurrence $C(1,2)$ is explored in Figs. 5 and 6, which shows a very similar behavior to the $C(1,4)$ case. Examining the dynamics of the next-nearest-neighbor concurrences $C(1,5)$ and $C(1,7)$ in the same way as we did with $C(1,2)$ and $C(1,4)$, we observed a very similar behavior with a much much smaller value of the concurrence, as expected for next nearest neighbors.

Figure 7 is used to check the behaviors of the system going from one magnetic field value to a smaller one and the reverse process. Both processes show the same characteristic oscillations, although they are different. The projection method requires mapping the ground state in $h = a$ into all the eigenstates of the system in $h = b$, whereas when we reverse the process, mapping becomes from the ground state in $h = b$ to all the eigenstates of the system in $h = a$. The behavior of the system is not mirrored.

No matter how we place the steps, all of them inevitably cause oscillation. This will be explained after we study all four kinds of external magnetic fields. But now we can answer the questions of what will happen to the entanglement of spins after the constant magnetic field is turned on and if we can benefit from that, say, by using the step magnetic field as an entanglement switch. The answer is negative because the entanglements oscillate fast and among relatively large values. A simple step magnetic field does not provide a way to control or tuning the entanglement in this spin system.

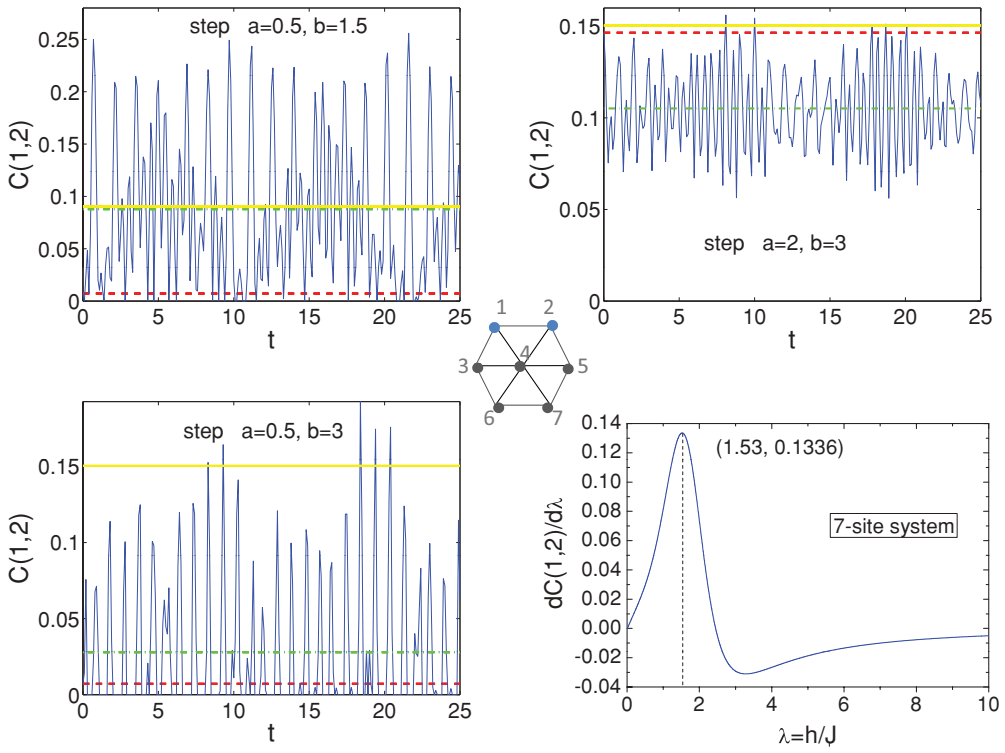

FIG. 5. (Color online) Dynamics of $C(1,2)$ (solid blue line) in the seven-site system when the step magnetic field is changed from $a = 0.5$ to $b = 1.5$ (before the critical point $h = 1.53$), from $a = 2$ to $b = 3$ (after), and from $a = 0.5$ to $b = 3$ (big step across the critical point), where time t is in units of J^{-1}, the dashed red line indicates the concurrence corresponding to a constant magnetic field $h = a$, the straight solid yellow line shows $h = b$, and the dot-dashed green line represents the average value of the oscillating concurrence.

B. Exponential magnetic field

The second kind of time-dependent magnetic field we will look at is the exponential one, which is represented by

$$h(t) = \begin{cases} a & t \leqslant t_0 \\ b + (a-b)e^{-\omega t} & t > t_0 \end{cases}. \tag{26}$$

It is a more general form than the step function; when $\omega \to \infty$, the exponential function turns into a step function. Figure 8 highlights the effect of ω on the concurrences $C(1,4)$ and $C(1,2)$. As one can see, the concurrence has the trend of following the shape of the exponential function, where it increases suddenly as the higher value is turned on and reaches a certain asymptotic equilibrium value. As the transition parameter ω increases, the concurrence shows an oscillation that increases rapidly as we further increase ω, where, in that case, the behavior resembles the step function case. It is interesting to see that the concurrence asymptotic equilibrium value, under the exponential magnetic field, coincides with the concurrence corresponding to the higher constant magnetic field, $h = b$ (the blue (red) straight line corresponds to $C(1,4)$ $[C(1,2)]$), which means that the two-dimensional Ising spin system shows an ergodic behavior in contrast to the one-dimensional system. In all cases the edge concurrence $C(1,2)$ is higher than the central one, $C(1,4)$, as expected as the latter shares the entanglement with a higher number of other spin pairs. Various a and b combinations are tested just as we did for the step function, with similar results to those in Fig. 8. Of course, changing the value of the final magnetic field leads to a change of the equilibrium value of the concurrence following it up and down. The concurrences $C(1,5)$ and $C(1,7)$ show very similar behavior to $C(1,2)$ and $C(1,4)$, as shown in Fig. 9, but with smaller magnitude.

In the sense of tuning entanglement, an exponentially changed magnetic field can be used to vary the entanglement from one value to another smoothly as long as long as its transition rate is slow enough. For instance, $\omega = 0.1$, that is, 10% of the interchange coupling J in the energy scale, is a good choice to accomplish this task, as we will explain later.

C. Hyperbolic magnetic field

As we have seen in the previous two sections, applying a step function or a rapid exponential function may disturb the system and lead to a strongly oscillating concurrence. Now let us apply another form of external magnetic field, namely, hyperbolic, which provides a smoother interaction with the system and reduces disturbances. The hyperbolic field is represented by

$$h(t) = \begin{cases} a & t \leqslant t_0 \\ \frac{(b-a)}{2}[\tanh(\omega t) + 1] + a & t > t_0 \end{cases}. \tag{27}$$

Figure 10 explores the behavior of the concurrences $C(1,4)$ and $C(1,2)$ of the system under the hyperbolic field at different transition constant values ω. Comparing the behavior of the concurrence in this case with the exponential case at the same frequencies, the similarity is clear, but with

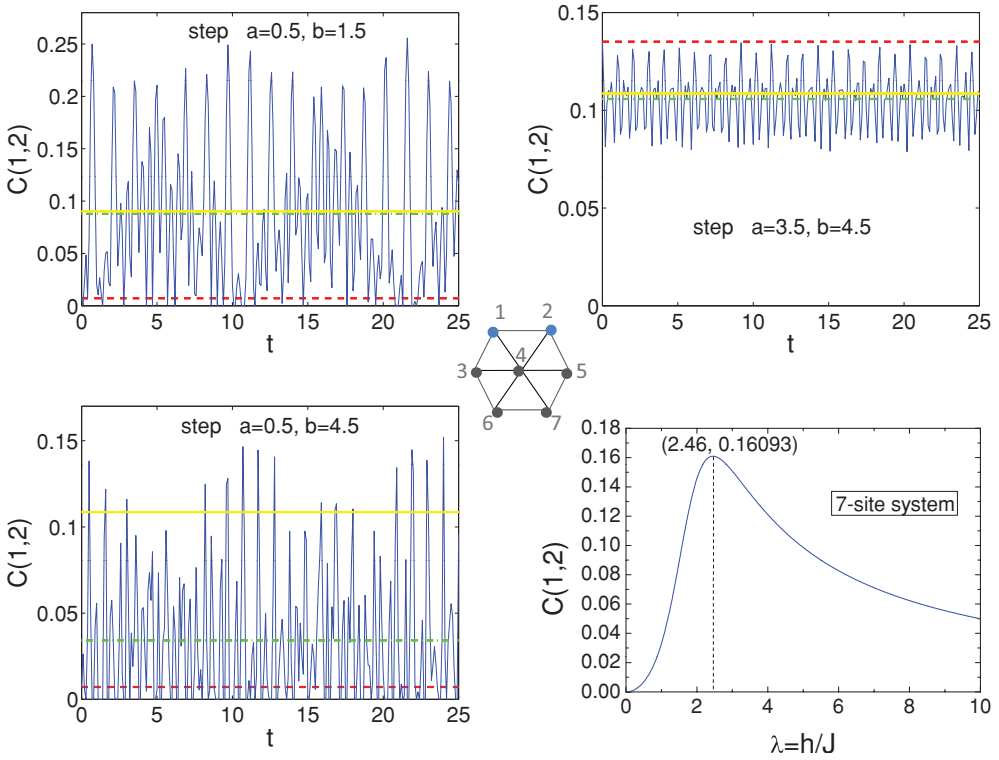

FIG. 6. (Color online) Dynamics of $C(1,2)$ (solid blue line) in the seven-site system when the step magnetic field is changed from $a = 0.5$ to $b = 1.5$ (before the maximum point $h = 2.46$), from $a = 3.5$ to $b = 4.5$ (after), and from $a = 0.5$ to $b = 4.5$ (big step across the maximum point), where time t is in units of J^{-1}, the dashed red line indicates the concurrence corresponding to a constant magnetic field $h = a$, the straight solid yellow line shows $h = b$, and the dot-dashed green line represents the average value of the oscillating concurrence.

much higher controllability for the hyperbolic field, with a sharper asymptotic concurrence value. The system confirms its ergodic behavior, as can be seen. Again, the next-nearest concurrences $C(1,5)$ and $C(1,7)$ show the same behavior as the nearest-neighbor concurrences, as shown in Fig. 11.

D. Periodic magnetic fields

In this section we test the dynamics of the system under a different form of external magnetic field, namely, periodic. It is represented by the sinusoidal function form

$$h(t) = \begin{cases} a & t \leqslant t_0 \\ a - a\sin(\omega t + \phi) & t > t_0 \end{cases}, \tag{28}$$

where ϕ represents an initial phase of the function, which determines the initial value of the applied magnetic field. For $\phi = 0$ we obtain a $\sin(\omega t)$ function, which is studied in Figs. 12 and 13, while for $\phi = \pi/2$ we get a $\cos(\omega t)$, which is explored in Figs. 14 and 15.

The influential factors in the sinusoidal field are amplitude a and angular frequency ω. Figure 12(b) is a good start to analyze them. When $\omega = 0.1$ and $a = 1$, both are small, and concurrence varies up and down in the same frequency as the field, but little dents and big catches come out as both ω and a increase, as shown in Figs. 12(c) and 12(d). As the frequency of the field increases, it becomes too fast for the system to follow, causing more imperfection in the concurrence oscillation. On the other hand, as we have seen in the previous magnetic field forms, larger magnetic fields do not necessarily bring larger concurrence, so dents appear as we increase a. Even larger magnetic fields totally break the pattern, as can be seen in Fig. 12(d). It is interesting to see that the larger amplitudes are not as disturbing to the nearest concurrences as they are to the next-nearest neighbors, as can be concluded from Fig. 13.

The critical effect of the initial phase, which determines the initial value of the field, can be seen in Figs. 14 and 15, where the phase was chosen to be $\pi/2$, resulting in a $\cos(\omega t)$ magnetic field. As one can see, the magnetic field is initially zero, and the concurrence is closely following the magnetic filed with a much sharper and much less distorted profile than the sine case. In fact, testing a middle value for the phase, between 0 and $\pi/2$, showed a concurrence with a middle profile between the sine and cosine cases (Fig. 16). Therefore, the smaller the initial value of the external magnetic field (best at zero) is, the less distorted the concurrence profile is.

IV. DYNAMICS OF THERMAL ENTANGLEMENT

In this section we intend to take a glance at the properties of entanglement in a many-body system at finite temperatures. The states describing a system in a thermal equilibrium state at absolute temperature T are determined by the Hamiltonian of the system and the inverse temperature $\beta = 1/kT$, where k is the Boltzmann constant. The thermal density matrix of the system is $\rho = Z^{-1}e^{-\beta H}$, where $Z = tr(e^{-\beta H})$ is the partition function of the system. Consider our step system and microstep

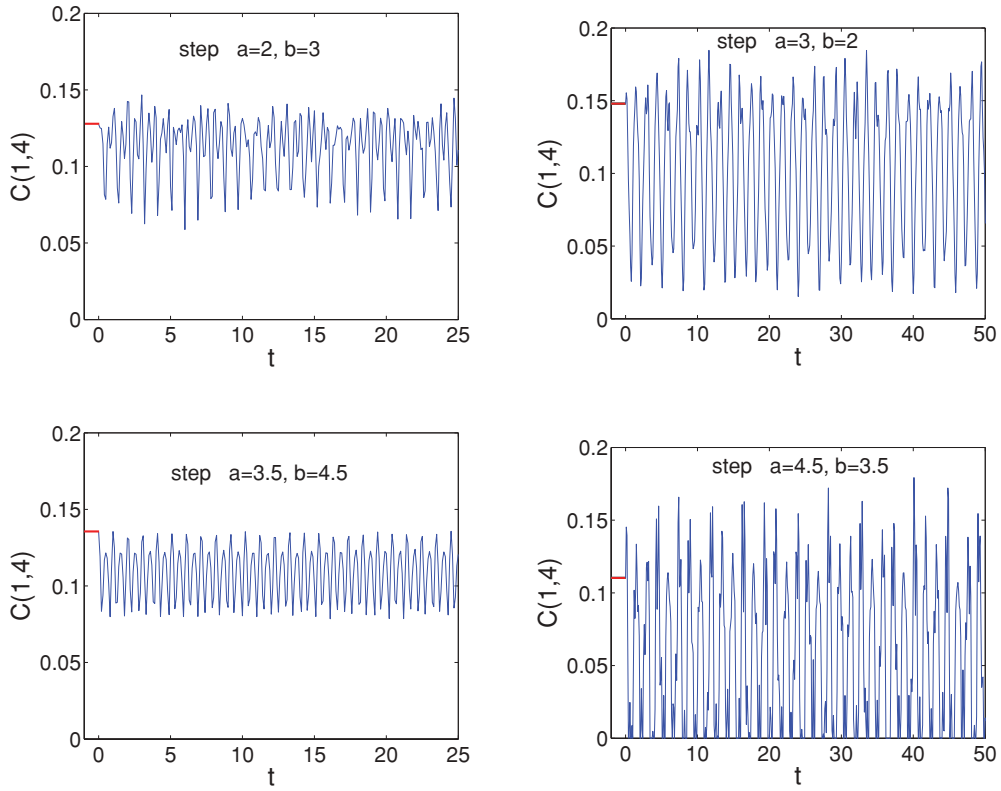

FIG. 7. (Color online) Dynamics of the system when changing from one magnetic field value to a smaller one and the reverse process, where the red straight line represents the concurrence of constant magnetic field $h = a$ before the step, the blue oscillating part represents concurrence behavior afterward, and time t is in units of J^{-1}.

system shown in Figs. 1 and 2, where any form of magnetic field can be represented by a sequence of step functions.

Assuming that the magnetic field has been divided into a sequence of steps, $a,b,c,\ldots,$ at times $t_0,t_1,t_2,\ldots,$ then at $t = t_0$, the system is in an initial equilibrium state described by

$$H(a) = -\sum_{<i,j>} \sigma_i^x \sigma_j^x - a\Sigma_i \sigma_i^z, \tag{29}$$

$$\rho(t_0) = \frac{\sum_i e^{-\beta E_i(a)} |\phi_i\rangle\langle\phi_i|}{\sum_i e^{-\beta E_i(a)}}. \tag{30}$$

At $t_1 > t_0$, the system evolves under the new magnetic field b, such that

$$H(b) = -\sum_{<i,j>} \sigma_i^x \sigma_j^x - b\Sigma_i \sigma_i^z, \tag{31}$$

$$\rho(t_1) = e^{-iH(b)(t_1-t_0)} \rho(0) e^{iH(b)(t_1-t_0)}. \tag{32}$$

Similarly, at $t_2 > t_1$, we have

$$H(c) = -\sum_{<i,j>} \sigma_i^x \sigma_j^x - c\Sigma_i \sigma_i^z, \tag{33}$$

$$\rho(t_2) = e^{-iH(c)(t_2-t_1)} \rho(t_1) e^{iH(c)(t_2-t_1)}. \tag{34}$$

Continuing in the same way along this sequence, we can obtain the density matrix at any time t, which can be used to evaluate the concurrence, as explained earlier.

One can see from the formulation that the thermal equilibrium (relaxation) only enters at $t = 0$, where we assume that the time scale of the dynamics under study is much smaller than the thermal relaxation time.

Figure 17 shows how concurrence evolves versus time and temperature under step magnetic field $h(t) = a$ at $t \leqslant t_0$, and $h(t) = b$ at $t > t_0$. Adjusting the step values leads to similar behaviors. They all oscillate through time, which is consistent with the results at zero temperature. When the temperature increases, oscillations keep the shape but are obviously weakened. As can be seen for either the step $a = 1$, $b = 2$ or the step $a = 2$, $b = 3$, the concurrence disappears around $kT = 1.75$. A value of $kT = 1.75$ means that when the energy associated with temperature is 1.75 times the exchange interaction J of the system, concurrence will be "killed," which shows how fragile the entanglement is in this spin system. Figures 18 and 19 show a very similar behavior for the concurrence of the system under other forms of the external magnetic field, namely, exponential and hyperbolic, respectively. The general profile of the concurrence resembles the zero-temperature case, especially at low temperatures. Remarkably, as the temperature increases, the concurrence decays very rapidly close to the zero temperature, as shown in Figs. 18(a) and 19(a), before it completely vanishes at about the same temperature as the exponential case [Figs. 18(b) and 19(b)].

To understand the critical temperature at which the concurrence vanishes better, we plot concurrence C vs temperature

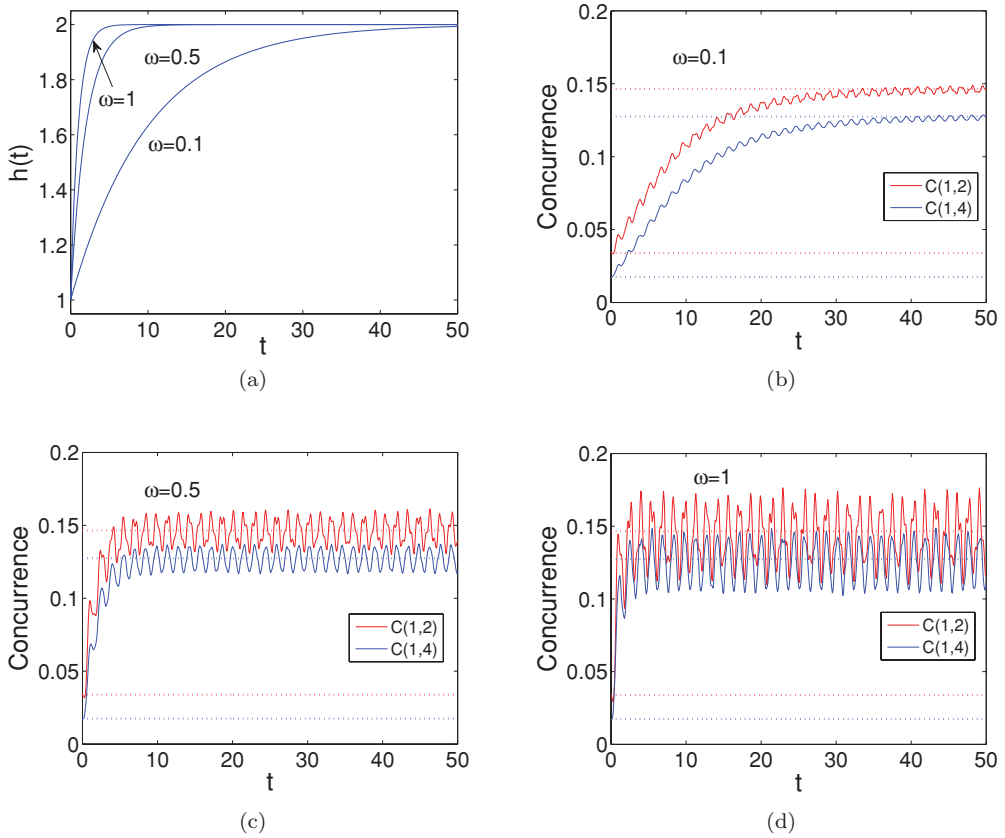

FIG. 8. (Color online) Dynamics of the concurrences $C(1,2)$ [solid red (upper) line] and $C(1,4)$ [solid blue (lower) line] in applied exponential magnetic fields for frequencies $\omega = 0.1, 0.5$, and 1, with strength $a = 1$, $b = 2$, where time t is in units of J^{-1}. The straight dotted red (upper) lines are concurrences $C(1,2)$ under constant magnetic field $a = 1$ and $b = 2$, and the dotted blue (lower) lines are for $C(1,4)$.

kT under certain constant magnetic field strength a (Fig. 20). As the magnetic field gets big, the critical temperature gets big too. When a is small, the zero temperature concurrence is small and stays stable as temperature increases for a while, but after a short time it drops dramatically. When a is close to the maximum point (Fig. 4), the zero-temperature concurrence is relatively large and drops all the way down as temperature increases. When a passes that point, as the concurrence becomes smaller and smaller, it has the ability to become more and more stable over the temperature change and finally becomes zero at relatively larger temperature. This tells us that sacrificing a certain amount of concurrence (choosing a large a) may make the concurrence more robust against thermal fluctuations.

In an attempt to understand the vanishing of concurrence, we found that if only the ground state doublets are included (others excluded by force), which are not exactly degenerate

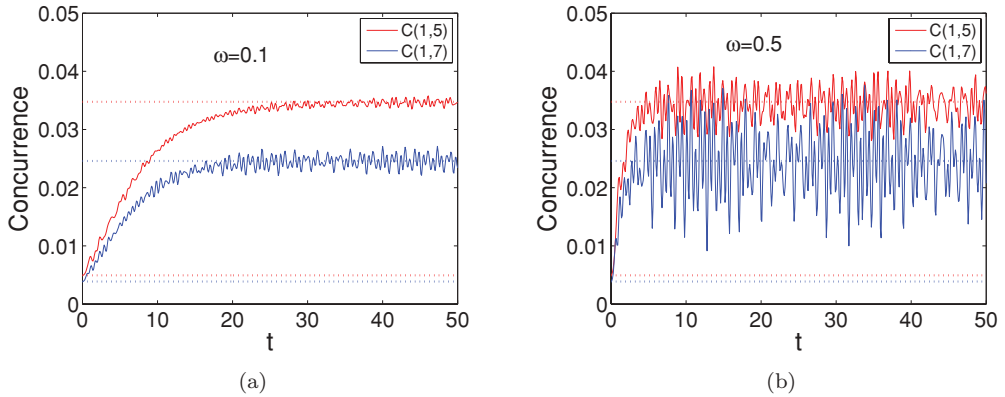

FIG. 9. (Color online) Dynamics of the concurrences $C(1,5)$ [solid red (upper) line] and $C(1,7)$ [solid blue (lower) line] in applied exponential magnetic fields of frequencies $\omega = 0.1$ and 0.5, with strength $a = 1$, $b = 2$, where time t is in units of J^{-1}. The straight dotted red (upper) lines are concurrences $C(1,5)$ under constant magnetic field $a = 1$ and $b = 2$, and the dotted blue(lower) lines are for $C(1,7)$.

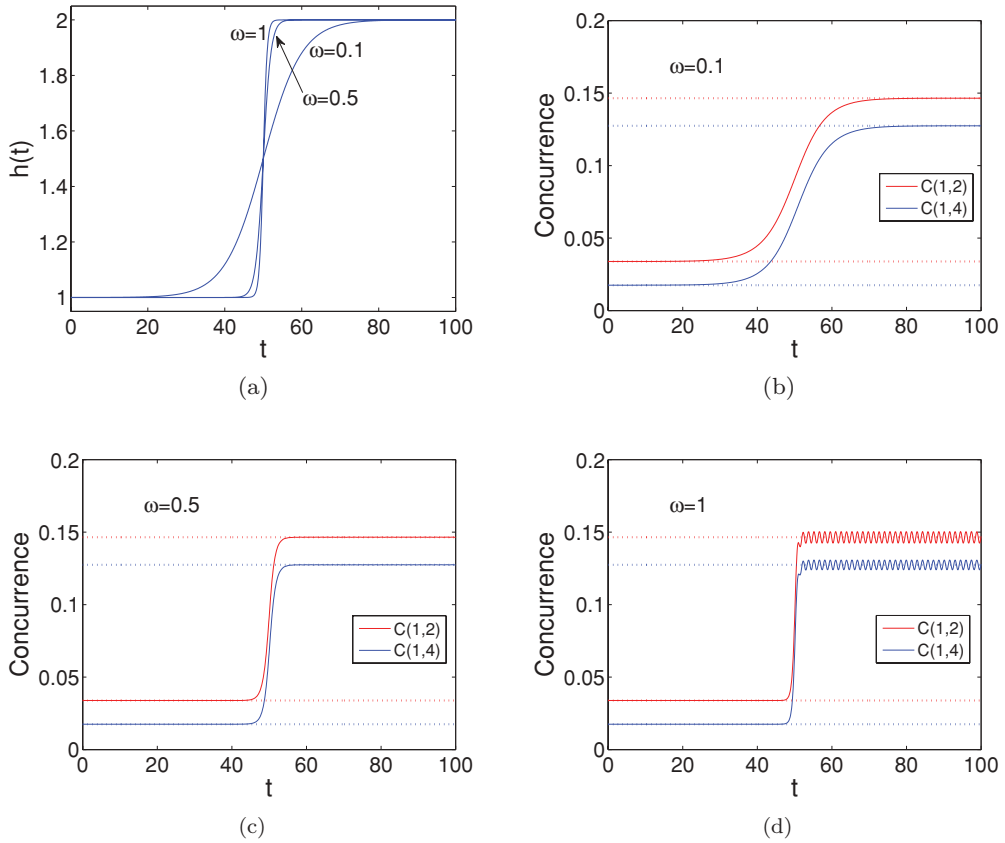

FIG. 10. (Color online) Dynamics of the concurrences $C(1,2)$ [solid red (upper) line] and $C(1,4)$ [solid blue (lower) line] in applied hyperbolic magnetic fields of frequencies $\omega = 0.1, 0.5$, and 1, with strength $a = 1$, $b = 2$, where time t is in units of J^{-1}. The straight dotted red (upper) lines are concurrences $C(1,2)$ under constant magnetic field $a = 1$ and $b = 2$, and the dotted blue (lower) lines are for $C(1,4)$.

due to the finite-size effect, the entanglement never vanishes at finite temperature. However, after the one-particle excitation continuum states are included, with higher-energy states projected out by force, the entanglement disappears at certain temperatures. This tells us that the mixing of the ground state and the low-energy excited states will cause the system to lose its entanglement. Physically, the population of the excited state n is determined by the ratio $(E_n - E_0)/T$ and remains almost zero for $T < E_n - E_0$ and becomes significantly nonzero as $T > E_n - E_0$. Therefore in the well-gapped regions (very small fields and large fields) the entanglement sustains the $T = 0$ values up to a certain T^* and then drops to zero, while in the critical region the entanglement starts dropping immediately after $T > 0$ without a plateau region. Numerically, however, T^* is, though related, not simply equal to the excitation gap. This might be so because the size of the system prevents it from revealing what only statistically holds true. Another question to be studied is why the concurrence

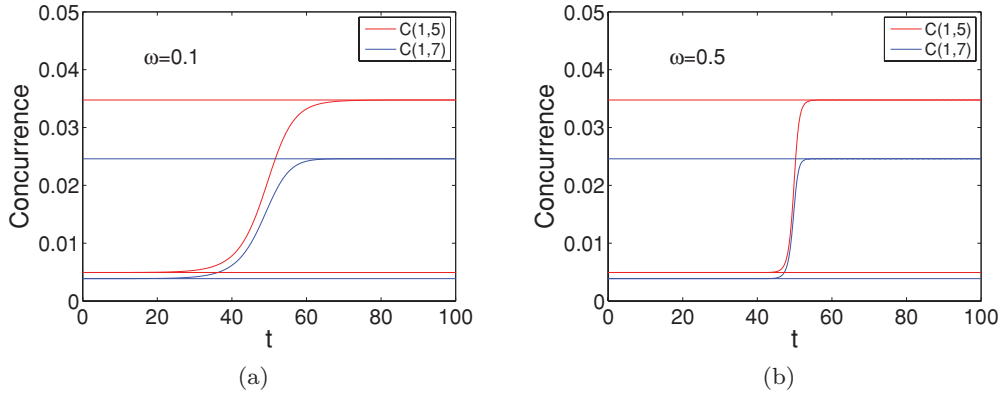

FIG. 11. (Color online) Dynamics of the concurrences $C(1,5)$ [solid red (upper) line] and $C(1,7)$ [solid blue (lower) line] in applied hyperbolic magnetic fields of frequencies $\omega = 0.1$ and 0.5, with strength $a = 1$, $b = 2$, where time t is in units of J^{-1}. The straight dotted red (upper) lines are concurrences $C(1,5)$ under constant magnetic field $a = 1$ and $b = 2$, and the dotted blue (lower) lines are for $C(1,7)$.

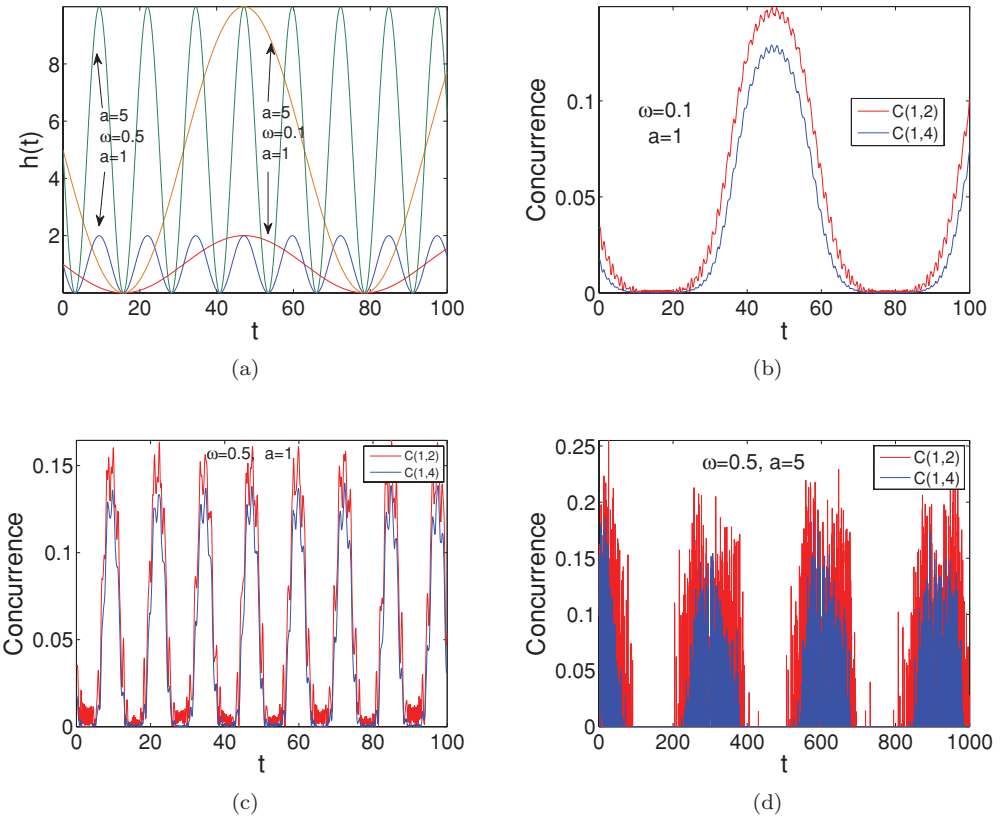

FIG. 12. (Color online) Dynamics of the concurrences $C(1,2)$ [red (upper) line] and $C(1,4)$ [blue (lower) line] in applied sine magnetic fields of various frequencies and field strength, $\omega = 0.1$ and $a = 1$, $\omega = 0.5$ and $a = 1$, and $\omega = 0.5$ and $a = 5$, where time t is in units of J^{-1}.

should come to zero in a "sudden" way like undergoing a phase transition, in contrast to an exponential decay, as one expects with a crossover.

V. FERMI'S GOLDEN RULE AND ADIABATIC APPROXIMATION

For all exponential, hyperbolic, and periodic forms, when the transition constant (frequency) ω is small, entanglement tends to follow the change of external magnetic field; when ω gets larger, entanglement gradually loses pace with the field. These phenomena can be explained by Fermi's golden rule and the adiabatic approximation. In order for the entanglement to follow the change in the external field, one requires that the system does not deviate far from the ground state, which is the adiabatic approximation.

Physically, it is equivalent to the requirement that the characteristic frequency in the external field is much smaller than the gap, $E_1(t) - E_0(t)$. This may be demonstrated in the following way. From time-dependent perturbation theory,

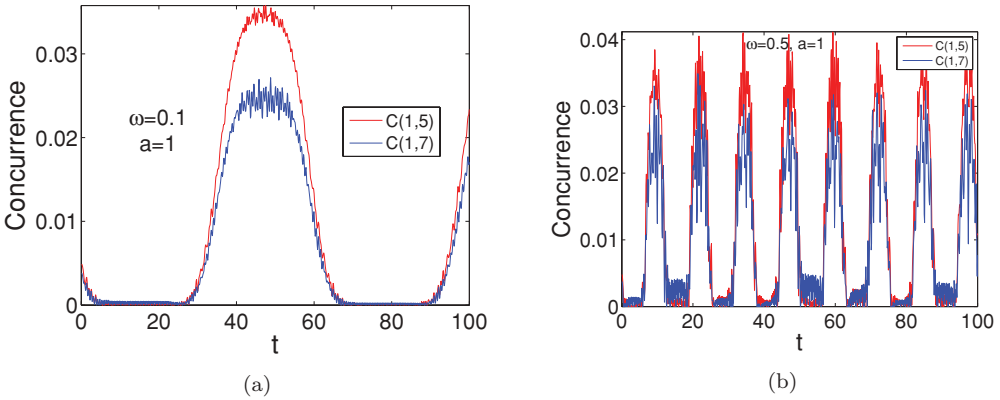

FIG. 13. (Color online) Dynamics of the concurrences $C(1,5)$ [red (upper) line] and $C(1,7)$ [blue (lower) line] in applied sine magnetic fields of various frequencies and field strength, $\omega = 0.1$ and $a = 1$ and $\omega = 0.5$ and $a = 1$, where time t is in units of J^{-1}.

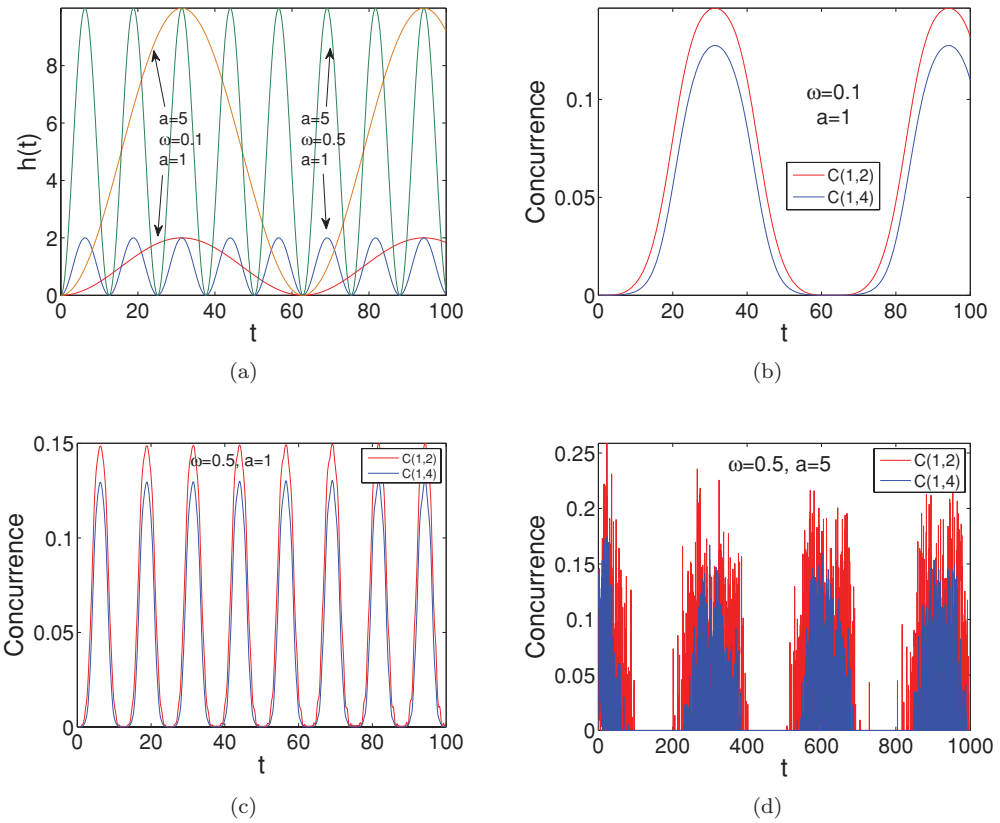

FIG. 14. (Color online) Dynamics of the concurrences $C(1,2)$ [red (upper) line] and $C(1,4)$ [blue (lower) line] in applied cosine magnetic fields of various frequencies and field strength, $\omega = 0.1$ and $a = 1$, $\omega = 0.5$ and $a = 1$, and $\omega = 0.5$ and $a = 5$, where time t is units of J^{-1}.

given a system at its ground state at $t = 0$, the probability amplitude of the nth state at $t > 0$ is given by

$$c_n(t) \approx \frac{-i}{\hbar} \int_0^t dt \langle n|H'(t)|0\rangle \exp\left(i(E_n - E_o)t\right). \quad (35)$$

The transition probability from ground state to the nth state is

$$P_{0n}(t) = \left|c_n(t)\right|^2 \approx \frac{\left|S^z_{n0}\right|^2}{\hbar^2} |h(E_n - E_0)|^2, \quad (36)$$

where we have

$$H'(t) = h(t) \sum_i \sigma_z^i = h(t) S^z, \quad (37)$$

$$h(\omega') = \int_{-\infty}^{\infty} h(t) \exp(i\omega' t) dt. \quad (38)$$

This is Fermi's golden rule, that the system only absorbs perturbations at frequencies that match the excitations energies. Data shown for both the exponential form and the harmonic

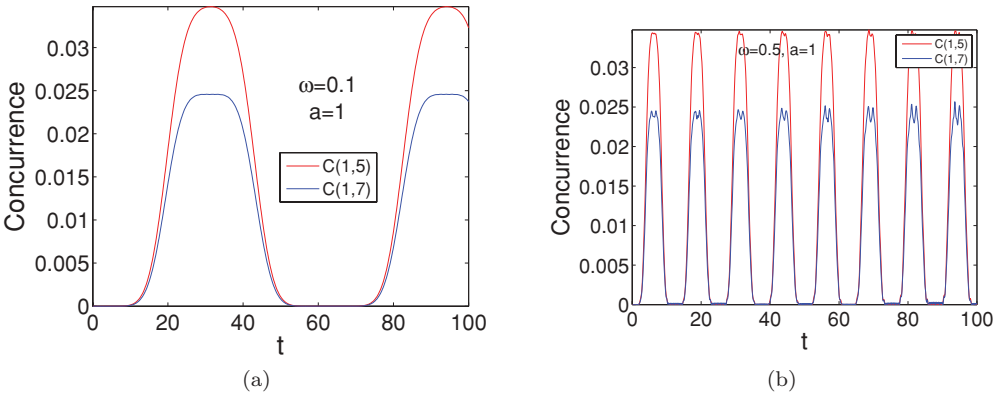

FIG. 15. (Color online) Dynamics of the concurrences $C(1,5)$ [red (upper) line] and $C(1,7)$ [blue (lower) line] in applied cosine magnetic fields of various frequencies and field strength, $\omega = 0.1$ and $a = 1$ and $\omega = 0.5$ and $a = 1$, where time t is in units of J^{-1}.

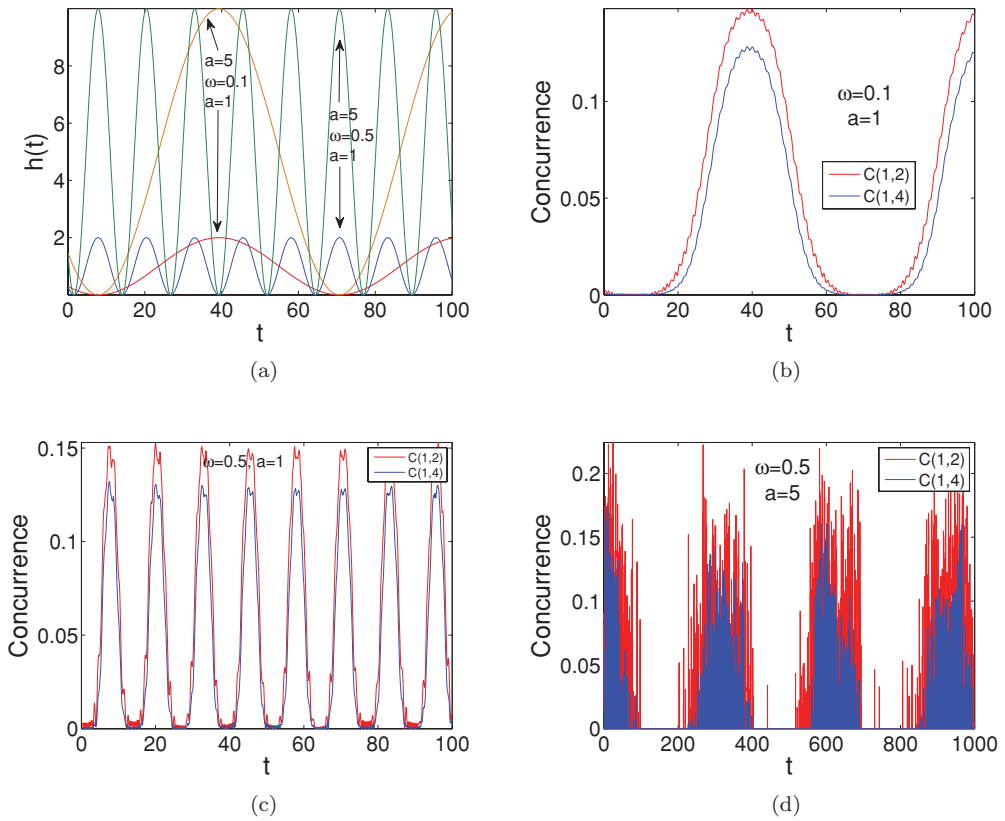

FIG. 16. (Color online) Dynamics of the concurrences $C(1,2)$ [red (upper) line] and $C(1,4)$ [blue (lower) line] in applied sinusoidal magnetic fields ($\phi = \pi/4$) of various frequencies and field strength, $\omega = 0.1$ and $a = 1$, $\omega = 0.5$ and $a = 1$, and $\omega = 0.5$ and $a = 5$, where time t is in units of J^{-1}.

form of the external field can be explained using this principle. For example, if one has

$$h(t) = \begin{cases} 1 & t \leqslant 0 \\ 1 - e^{-\omega t} & t > 0 \end{cases}, \tag{39}$$

Fourier transform gives

$$|h(\omega')|^2 = \frac{1}{(\omega'^2 + \omega^2)}. \tag{40}$$

The transition probability is

$$P_{0n} \approx \frac{\left|S^z_{n0}\right|^2}{\hbar^2} \frac{1}{(\omega'^2 + \omega^2)}. \tag{41}$$

From this formula we can see that if one has $\omega \ll E_1 - E_0$, the transition rate is very small, and the system is able to follow the change of the magnetic field.

The validity of the adiabatic approximation may fail in two cases. First, when the external field is changing too quickly for the system to follow, say, $\omega \gg E_n - E_0$ for certain n, the

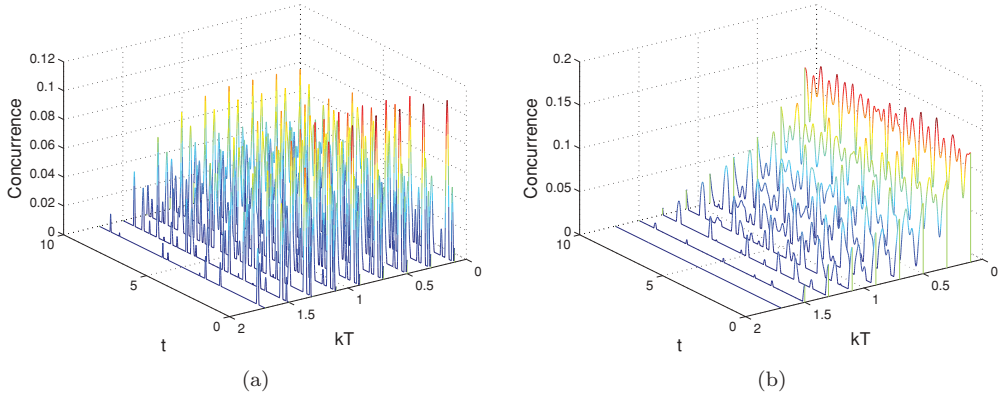

FIG. 17. (Color online) The time evolution of the concurrence $C(1,4)$ as a function of the temperature kT under an applied step magnetic field (a) $a = 1$, $b = 2$ and (b) $a = 2$, $b = 3$, where time t is in units of J^{-1} and kT is in units of J.

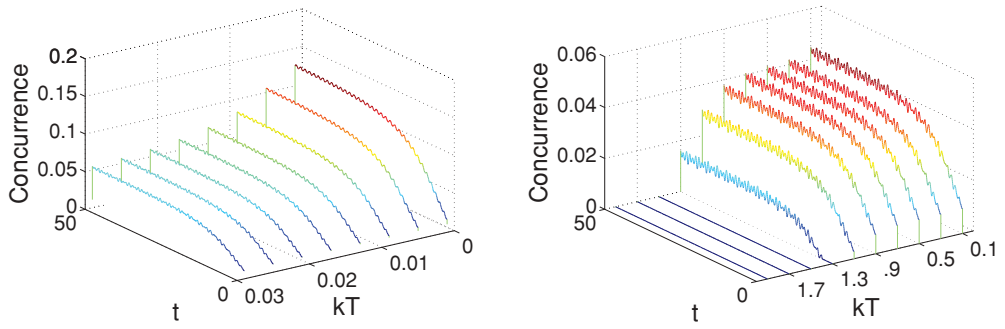

FIG. 18. (Color online) The time evolution of the concurrence $C(1,4)$ as a function of the temperature kT, (a) kT from 0 to 0.03 and (b) kT from 0.1 to 2, under an applied exponential magnetic field, where time t is in units of J^{-1} and kT is in units of J.

system has a significant probability of being excited to the nth state, thus losing the ground-state entanglement. One can see this type of breaking for the exponential (hyperbolic) form of the external field with large ω and for a step function (which corresponds to $\omega \to \infty$ of the exponential form) and for the case of harmonic field with high frequency. The second type of adiabatic approximation breaking takes place if the strength of the external field is too strong, so that during its change, the system has to cross its phase boundary. Suppose the system is able to follow the field and stays on the ground state up to the critical field, then right at the transition the gap between the ground state and a one-particle excitation continuum is closing; therefore an arbitrarily slow field can significantly send the system to various excited states. Although this picture is, in principle, more relevant in the thermodynamic limit than for the small-sized system in the current study, this type of adiabatic breaking is still observed in Figs. 12(d) and 14(a).

VI. EXTENSION OF PROJECTION METHOD TO LARGER SYSTEMS

At the end of Sec. II D, we mentioned that the summation of Eq. (19) covers all the eigenstates. For large systems, such as a 19-site system, this step is not realistic. Now if we consider a system at zero temperature and at $t = 0$, one starts to change the field. One can prove that not all excited states need to be included in the projection because most excited states have zero overlap with the ground state by symmetry. The global symmetries of the system are spatial sixfold rotation C_6, spin-flip operation Z_2, and spatial reflection about the x axis m_x and the y axis m_y. Group theory tells us that the Hamiltonian can be block diagonalized and that each block corresponds to an irreducible representation of the symmetry group. If the ground state lies in the ith block, then since the time-evolution operator $U(t) = T\exp[-i\int_0^t H(t)dt]$ commutes with all symmetry operators, the end state $|\psi(t)\rangle$ still lies in the same irreducible representation. Let us illustrate this idea by considering a simpler symmetry group constituted by only C_6 and Z_2; then the group has 12 one-dimensional irreducible representations. Each representation corresponds to the eigenvalues of the two operators: $[(-1)^m, \exp(i\frac{n\pi}{3})]$, where $m = 1,2$ and $n = 1,2,\ldots,6$. Suppose $|\psi_0\rangle$ belongs to the sector denoted by (m,n) and $|\phi_{m'n'}(t)\rangle$ is an eigenstate of $H(t)$ in the (m',n') sector. Then we have

$$[C_6, U(t)] = 0, \tag{42}$$

$$\langle\phi_{m'n'}(t)|[C_6, U(t)]|\psi(0)\rangle = (e^{im'\pi/3} - e^{im\pi/3})\langle\phi_{m'n'}|\psi(t)\rangle = 0. \tag{43}$$

Therefore the overlap is nonzero only if $m' = m$. Similarly, we can prove $n' = n$. The simplified symmetry group can divide the original Hilbert space (unequally) into 12 parts, and the dynamics is fully captured in only one of them; the additional $m_{x,y}$ symmetries can help further reduce the number of states one needs to consider for the zero-temperature dynamics.

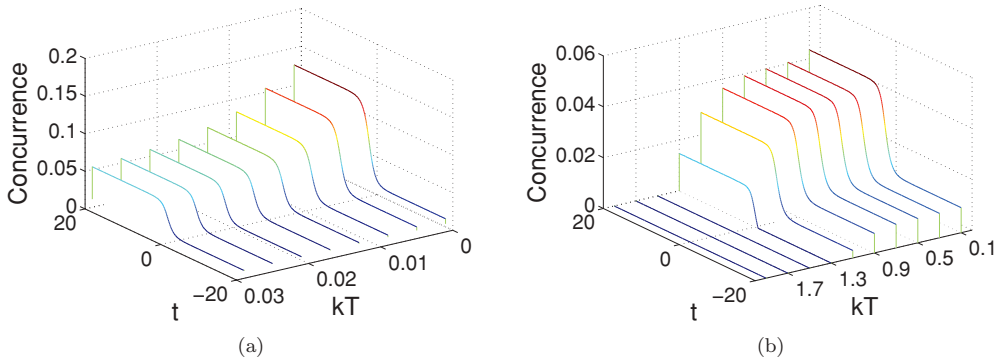

FIG. 19. (Color online) The time evolution of the concurrence $C(1,4)$ as a function of the temperature kT, (a) kT from 0 to 0.03 and (b) kT from 0.1 to 2, under an applied hyperbolic magnetic field, where time t is in units of J^{-1} and kT is in units of J.

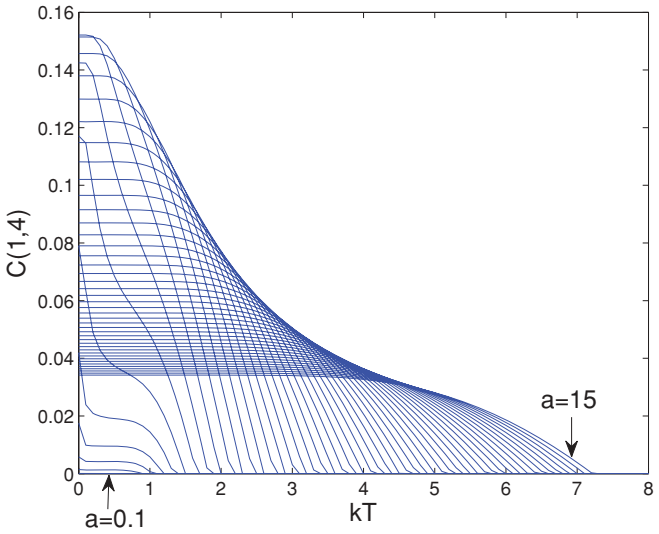

FIG. 20. (Color online) Concurrence $C(1,4)$ vs temperature at certain constant magnetic field strength a, where a varies from 0.1 to 15 in units of J.

Although symmetry has helped to largely reduce the calculation cost, the remaining problem may still be too extensive to solve. It is reasonable to apply an approximation: only states that have energies that are not much higher than the ground state are included in the projection if the external field does not vary too quickly. Consider the case when the field changes very slowly; hence the adiabatic approximation is valid, and one needs to include only the ground state in the calculation. Further, if the field changes faster than the excitation gap but not as fast as ranging the whole excitation spectrum, it would be enough if one only includes the first few excited states (possibly the first band of excitations) to cover the most important time scales.

VII. CONCLUSION AND FUTURE DIRECTIONS

We have investigated the dynamics of entanglement in a two-dimensional triangular Ising spin lattice in an external time-dependent magnetic field. The spins are coupled to each other through nearest-neighbor exchange interaction. We studied nearest-neighbor and next-nearest-neighbor concurrences of the system under different time-dependent forms of the external magnetic field: step, exponential, hyperbolic, and periodic. In contrast to the one-dimensional Ising spin system, the two-dimensional system shows an ergodic behavior under the effects of the time-dependent magnetic fields. The step magnetic field causes a great disturbance to the system and leads to a rapidly oscillating concurrence with amplitude and frequency that depend on the magnetic field step values. The system shows more controllability under the effects of the other forms of magnetic fields where the concurrence profile follows the shape of the applied magnetic field very closely, particularly for a small magnetic field strength and a small transition constant for the exponential and hyperbolic fields and frequency for the periodic field. As the values of these parameters increase, the concurrence breaks the pattern, and rapid oscillations take place. The initial value of the applied periodic field, independent of the amplitude, is very critical to the oscillating concurrence profile, and a smaller initial value yields a less distorted oscillation. Studying the entanglement at zero and finite temperature revealed that it sustains the same profile under the different magnetic fields as the temperature increases but with reduced magnitude. The effect of the temperature is very devastating to the entanglement of the system, which decays rapidly as the temperature increases. Interestingly, though a large value of the magnetic field strength leads to a small concurrence, it is found to be more robust against thermal fluctuations than the smaller field strength. In the future, we would like to study a larger-size two-dimensional spin lattice to examine the effect of the size on the different properties of the system [36]. Also we would like to study a more generalized spin system where the coupling among the spins in the other directions, rather than the z direction, is taken into account along with the effect of a time-dependent exchange coupling.

Furthermore the dynamics of a real system is determined not only by its internal Hamiltonian but also by its environment. The rich and varied physics of spin systems make spin baths fundamentally interesting [37]. We plan to study the reduced dynamics of the center spin with the rest as the environment and also entanglements and decoherence for a reduced system with two interacting spins with the rest as the environment in the 7- and 19-site spin systems.

ACKNOWLEDGMENTS

We are grateful to the Army Research Office (ARO) for supporting this work at Purdue and to the Deanship of Scientific Research for support at King Saud University.

[1] A. Peres, *Quantum Theory: Concepts and Methods* (Kluwer, Dordrecht, 1993).

[2] S. Kais, in *Reduced-Density-Matrix Mechanics—With Application to Many-Electron Atoms and Molecules*, Advances in Chemical Physics Vol. 134 (Wiley, New York, 2007), pp. 493–535.

[3] S. L. Sondhi, S. M. Girvin, J. P. Carini, and D. Shahar, Rev. Mod. Phys. **69**, 315 (1997).

[4] T. J. Osborne and M. A. Nielsen, Phys. Rev. A **66**, 032110 (2002).

[5] J. Zhang, F. M. Cucchietti, C. M. Chandrashekar, M. Laforest, C. A. Ryan, M. Ditty, A. Hubbard, J. K. Gamble, and R. Laflamme, Phys. Rev. A **79**, 012305 (2009).

[6] O. Osenda, Z. Huang, and S. Kais, Phys. Rev. A **67**, 062321 (2003).

[7] Z. Huang, O. Osenda, and S. Kais, Phys. Lett. A **322**, 137 (2004).

[8] M. Nielsen and I. Chuang, *Quantum Computation and Quantum Communication* (Cambridge University Press, Cambridge, 2000).

[9] *The Physics of Quantum Information: Quantum Cryptography, Quantum Teleportation, Quantum Computing*, edited by D. Boumeester, A. Ekert, and A. Zeilinger (Springer, Berlin, 2000).
[10] A. Barenco, D. Deutsch, A. Ekert, and R. Jozsa, Phys. Rev. Lett. **74**, 4083 (1995).
[11] L. Vandersypen, M. Steffen, G. Breyta, C. Yannoni, M. Sherwood, and I. Chuang, Nature (London) **414**, 883 (2001).
[12] I. L. Chuang, N. Gershenfeld, and M. Kubinec, Phys. Rev. Lett. **80**, 3408 (1998).
[13] J. Jones, M. Mosca, and R. Hansen, Nature (London) **393**, 344 (1998).
[14] J. I. Cirac and P. Zoller, Phys. Rev. Lett. **74**, 4091 (1995).
[15] Q. A. Turchette, C. J. Hood, W. Lange, H. Mabuchi, and H. J. Kimble, Phys. Rev. Lett. **75**, 4710 (1995).
[16] D. V. Averin, A. N. Korotkov, A. J. Manninen, and J. P. Pekola, Phys. Rev. Lett. **78**, 4821 (1997).
[17] Q. Wei, S. Kais, and Y. P. Chen, J. Chem. Phys. **132**, 121104 (2010).
[18] W. Zurek, Phys. Today **44**, 36 (1991).
[19] P. W. Shor, Phys. Rev. A **52**, R2493 (1995).
[20] D. Bacon, J. Kempe, D. A. Lidar, and K. B. Whaley, Phys. Rev. Lett. **85**, 1758 (2000).
[21] D. P. DiVincenzo, D. Bacon, J. Kempe, G. Burkard, and K. B. Whaley, Nature (London) **408**, 339 (2000).
[22] S. Doronin, E. Fel'dman, and S. Lacelle, Chem. Phys. Lett. **353**, 226 (2002).
[23] J. Lages, V. V. Dobrovitski, M. I. Katsnelson, H. A. De Raedt, and B. N. Harmon, Phys. Rev. E **72**, 026225 (2005).
[24] Z. Huang and S. Kais, Int. J. Quantum. Inf. **3**, 483 (2005).
[25] Z. Huang and S. Kais, Phys. Rev. A **73**, 022339 (2006).
[26] G. Sadiek, B. Alkurtass, and O. Aldossary, Phys. Rev. A **82**, 052337 (2010).
[27] E. Lieb, T. Schultz, and D. Mattis, Ann. Phys. **16**, 407 (1961).
[28] S. Sachdev, *Quantum Phase Transitions* (Cambridge University Press, Cambridge, 2001).
[29] J. C. Xavier, Phys. Lett. B **81**, 224404 (2010).
[30] J. Silva-Valencia, J. C. Xavier, and E. Miranda, Phys. Rev. B **71**, 024405 (2005).
[31] F. Capraro and C. Gros, Eur. Phys. J. B **29**, 35 (2002).
[32] Q. Xu, S. Kais, M. Naumov, and A. Sameh, Phys. Rev. A **81**, 022324 (2010).
[33] C. Cohen-Tannoudji, B. Diu, and F. Laloë, *Quantum Mechanics* (Wiley, 2005).
[34] A. Osterloh, L. Amico, G. Falci, and R. Fazio, Nature (London) **416**, 608 (2002).
[35] W. K. Wootters, Phys. Rev. Lett. **80**, 2245 (1998).
[36] S. Kais and P. Serra, in Advances in Chemical Physics Vol. 125 (Wiley, New York, 2003), pp. 1–99.
[37] G. Sadiek, Z. Huang, O. Aldossary, and S. Kais, Mol. Phys. **106**, 1777 (2008).